

# Cyclic Dichalcogenides Extend the Reach of Bioreductive Prodrugs to Harness Thiol/Disulfide Oxidoreductases: Applications to *seco*-Duocarmycins Targeting the Thioredoxin System

Jan G. Felber, Annabel Kitowski, Lukas Zeisel, Martin S. Maier, Constanze Heise, Julia Thorn-Seshold, and Oliver Thorn-Seshold\*



Cite This: *ACS Cent. Sci.* 2023, 9, 763–776



Read Online

ACCESS |



Metrics & More

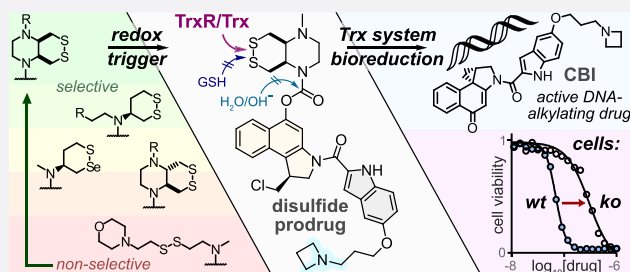


Article Recommendations



Supporting Information

**ABSTRACT:** Small-molecule prodrug approaches that can activate cancer therapeutics selectively in tumors are urgently needed. Here, we developed the first antitumor prodrugs designed for activation by thiol-manifold oxidoreductases, targeting the thioredoxin (Trx) system. The Trx system is a critical cellular redox axis that is tightly linked to dysregulated redox/metabolic states in cancer, yet it cannot be addressed by current bioreductive prodrugs, which mainly cluster around oxidized nitrogen species. We instead harnessed Trx/TrxR-specific artificial dichalcogenides to gate the bioactivity of 10 “off-to-on” reduction-activated duocarmycin prodrugs. The prodrugs were tested for cell-free and cellular reductase-dependent activity in 177 cell lines, establishing broad trends for redox-based cellular bioactivity of the dichalcogenides. They were well tolerated *in vivo* in mice, indicating low systemic release of their duocarmycin cargo, and *in vivo* anti-tumor efficacy trials in mouse models of breast and pancreatic cancer gave promising indications of effective tumoral drug release, presumably by *in situ* bioreductive activation. This work therefore presents a chemically novel class of bioreductive prodrugs against a previously unaddressed reductase chemotype, validates its ability to access *in vivo*-compatible small-molecule prodrugs even of potentially cumulative toxins, and so introduces carefully tuned dichalcogenides as a platform strategy for specific bioreduction-based release.



## 1. INTRODUCTION

Classic cancer chemotherapy, treating tumors with cytotoxic drugs against ubiquitous critical biological targets (DNA integrity, cell division, etc.), incurs severe systemic side effects from unspecific drug distribution to healthy tissues whose function also depends on these targets. Prodrug concepts can deliver an additional layer of control over drug activity beyond simple biodistribution, and tumor-preferential mechanisms for drug unmasking—e.g., small-molecule<sup>1</sup> or antibody-directed<sup>2</sup> approaches—are intensively pursued.

Bioreductive prodrugs are enzymatically unmasked *in situ* by reduction.<sup>3</sup> Reductive processes are especially prominent in hypoxic environments, such as tumors, since re-oxidation of metastable intermediates is hindered. Thus, bioreductive prodrugs are sometimes termed “hypoxia-activated”. They are in active development, and several reached phase III clinical trials. However, only a small biological target space and a correspondingly restricted small chemical space have been explored for bioreductive prodrugs, which is a missed opportunity for innovative therapeutics (Figure 1a). The first class developed were natural product quinones, activated by ubiquitous quinone reductases, such as the mitomycins and their synthetic analogues (e.g., apaziquone<sup>4</sup>). Later, oxidized nitrogen species that can be reduced by a broader range of

enzyme classes came to dominate designs, including (i) aliphatic *N*-oxides that are reduced to basic amines, which can trigger DNA binding (AQ4N/banoxantrone<sup>5</sup>); (ii) aromatic *N*-oxides that are reduced to bioactive nitrogenous bases (tirapazamine<sup>6</sup>); and (iii) nitroaryls, that after reduction can eliminate a drug (TH-302/Evofosfamide<sup>7</sup>), or nucleophilically assist reaction mechanisms (PR-104<sup>8</sup>), or dock to targets (nitracrine<sup>9</sup>) (Figure 1a). However, no cancer prodrug using these oxidized nitrogen chemotypes and their targets has been approved,<sup>10</sup> and novel, modular strategies to bioreductively activate drugs specifically inside tumors are required.

The thioredoxin system, composed of the thioredoxins (Trxs) and their NADPH-dependent reductases (TrxRs), are enzymatic reductants that are central to redox homeostasis, cellular metabolism, DNA synthesis, protein folding, and antioxidant response.<sup>11</sup> Overactivity of the thioredoxin system

Received: December 8, 2022

Published: March 28, 2023



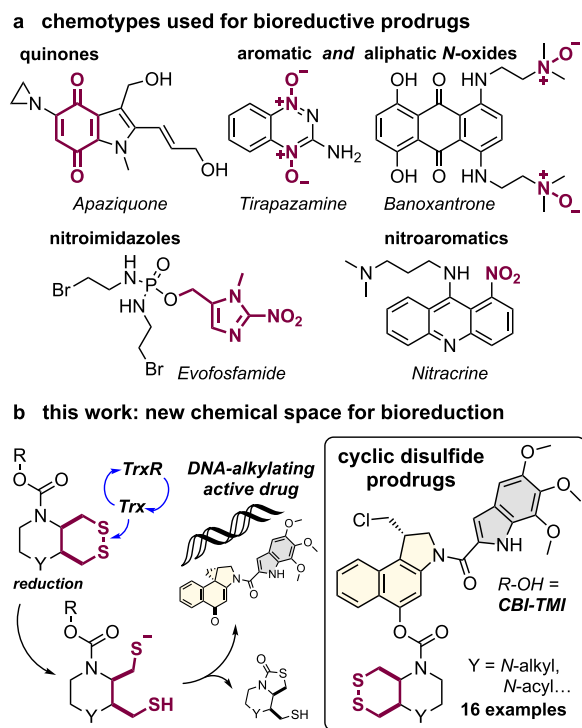


**Figure 1. Bioreductive prodrugs.** (a) Chemotypes used for bioreductive clinical prodrugs: (i) aliphatic N-oxides, (ii) aromatic N-oxides, and (iii) nitroimidazoles and nitroaromatics. (b) Bicyclic disulfides targeting the Trx/TrxR system, one of the new motifs for bioreductive prodrug development introduced in this paper.

is strongly implicated in cancer progression,<sup>12</sup> and Trx expression is often upregulated in tumors.<sup>13</sup> This may offer a

unique point of chemical attack: Trx is the cell's strongest dithiol-based reductant, so reduction-resistant substrates, that are selectively but only slowly activated by Trx under physiological conditions, might be faster activated by Trx in diseased tissues. However, bioreductive prodrug approaches for the Trx system have not yet been designed.

Chemically, Trx/TrxR are dithiol/selenolthiol reductases that can address protein as well as small-molecule disulfides. The biological target space tested by (any) disulfide-based prodrugs has remained limited, as essentially only GSH-labile non-specific linear disulfides<sup>14</sup> and 1,2-dithiolanes<sup>15,16</sup> have been examined. Recently, we have developed sets of 6-membered cyclic dichalcogenides with unique reduction-resisting properties as well as reductase selectivity profiles.<sup>17–19</sup> Stabilized disulfides in these series were selectively activated by Trxs, with excellent resistance to even thousand-fold higher levels of GSH and monothiols,<sup>17</sup> and bifunctional bicyclic disulfides permitted drastic enhancement of their reductive activation kinetics.<sup>19</sup> Cyclic selenenyl sulfides instead had a selenium-preferring, regioisomer-dependent activation mechanism, making them excellently selective substrates for TrxR1 in live cells.<sup>18,20</sup> These bioreductive motifs were validated in fluorogenic probes in acute applications (minutes to hours) in cell culture. However, it is unknown whether such designs can be useful for long-term redox-selective drug delivery, particularly in the context of cancer, for which their Trx/TrxR targets' biology is most relevant (Figure 1b) since *in vivo* uses are more stringent, e.g., requiring them to also resist activation by hydrolytic or oxidative metabolism in the long term.

The duocarmycins are DNA alkylators with high potency across a broad range of cell lines<sup>21</sup> that have excellent characteristics as modular payloads for cytotoxic anticancer

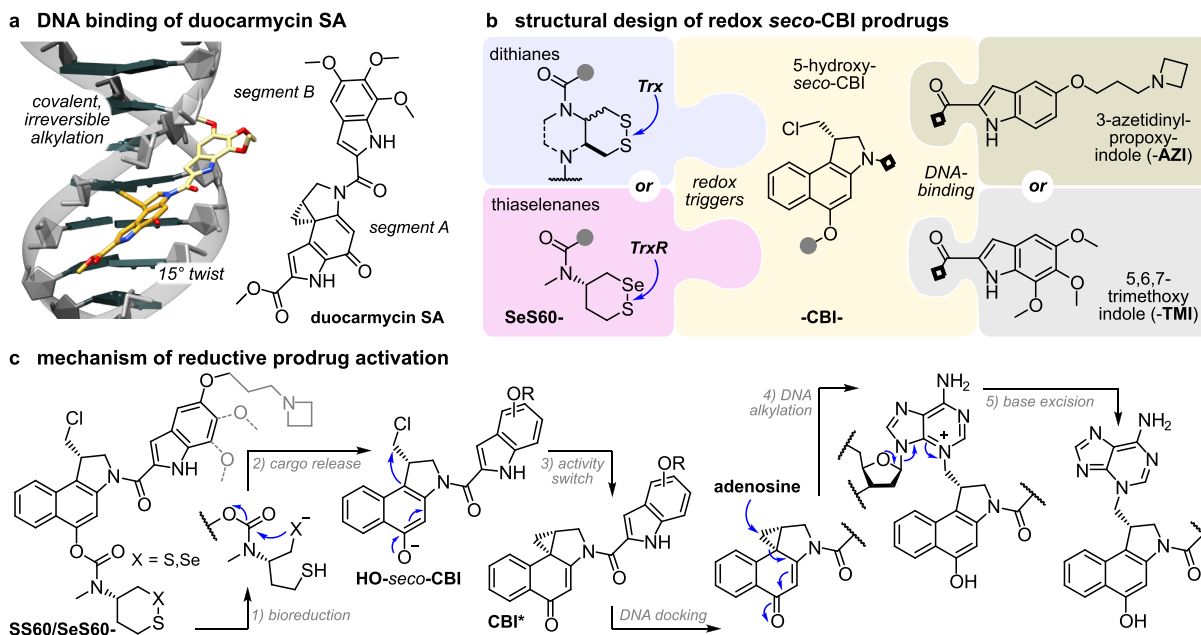


**Figure 2. *seco*-Duocarmycin prodrug design and mechanism of activation.** (a) DNA docking by duocarmycin SA with a 15° amide twist that initiates DNA alkylation (PDB: 1DSM). (b) Our three-part bioreductive prodrug design: (i) an enzyme-selective dithiane/thiaselenane masks (ii) the *seco*-CBI phenol to which (iii) an indole segment is attached for DNA binding and/or solubility. Prodrugs are named by parts, e.g., SeS60-CBI-AZI (thiaselenane trigger SeS60, -CBI-, and 3-azetidyl-propoxy-indole -AZI). (c) Reductive activation: (1) enzymatic bioreduction; (2) cyclization of the reduced chalcogenide to expel the CBI phenolic leaving group; (3) bioactivity switch: intramolecular Winstein cyclization to create the activated cyclopropane; (4) DNA docking, leading to DNA alkylation; and (5) base excision, irreversible DNA damage, and apoptosis.<sup>35</sup>

prodrugs.<sup>22</sup> Their key motif is an activated cyclopropane electrophile, which can be generated *in situ* from a biologically inactive *seco*-precursor by unmasking a phenol or aniline that then spontaneously undergoes phenylogous cyclization (Figure 2).<sup>23</sup> Due to this elegant off-to-on bioactivity switch, synthetic *seco*-duocarmycin-type prodrugs have been broadly developed as stimulus-responsive proagents, often harnessing the simpler cyclopropabenz[indole] (CBI)<sup>24,25</sup> alkylator and the minimal 5,6,7-trimethoxyindole (TMI)<sup>26</sup> DNA binder motifs.<sup>26</sup> Hydrolyase-unmaskable phenolic substrates such as esters, carbamates,<sup>27,28</sup> and glycosides<sup>29,30</sup> have been broadly applied. Bioreductive substrates aiming at increased tumor specificity have also been tested, including nitro-*seco*-CBIs as aniline precursors<sup>31,32</sup> and *N*-acyl-*O*-amines as phenol precursors.<sup>33,34</sup> The modular “puzzle” design of *seco*-duocarmycins, combining a DNA binder with an electrophile segment and its unmaskable trigger, sets up a platform approach for prodrug development (Figure 2b).

Aiming to test the potential of Trx/TrxR-responsive cyclic dichalcogenides as trigger units that may open new chemical space as well as new target spaces for bioreductive prodrugs, we now design and test a suite of 10 redox-responsive CBI-based therapeutic prodrugs based on cyclic dichalcogenides (Figure 2).

## 2. RESULTS AND DISCUSSION

### 2.1. Modular Design Logic for Dichalcogenide Prodrugs

We aimed at modular prodrug designs, separating the Trx/TrxR-bioreducible trigger module from its duocarmycin cargo module. This design also separates the functional steps responsible for bioactivity (Figure 2c): (1) bioreduction of the trigger by dithiol or selenolthiol reductases, e.g., Trx<sup>17</sup> or TrxR;<sup>18</sup> (2) *S*-*exo*-*trig* cyclization by the trigger to release the (biologically inactive) duocarmycin phenolic cargo; (3) 1,4-nucleophilic Winstein cyclization<sup>36</sup> to create the activated cyclopropane CBI\*; (4) CBI\* docking in the DNA minor groove while twisting its aryl–aryl plane, and the now more activated cyclopropane irreversibly alkylating adenosine at the N3-position;<sup>37</sup> and (5) spontaneous excision of the quaternized purine base, causing DNA damage and ultimately cell death.

We expected that varying trigger and cargo motifs would clarify the separate contributions of reduction and of drug sensitivity to the overall prodrug efficacy, thus setting a rational basis both for further tuning of dichalcogenide triggers as well as for their adaptation to alternative bioactive cargos.<sup>38</sup> This is because, in our model (Figure 2c), the trigger mainly determines the rate or degree of cargo release, by controlling reduction and cyclization rates (steps 1–2), whereas the cargo mainly determines the expected potency for a particular degree of drug release, by controlling the speed of cyclopropane formation and likelihood of DNA binding/alkylation (steps 3–4).

We therefore planned to use a range of dichalcogenide redox triggers (e.g., dithiane SS60-) to covalently mask hydroxy-*seco*-CBI (-CBI-) by a stable tertiary carbamate linkage<sup>39,40</sup> while varying the DNA-binding indoles that complete the duocarmycins to modulate the ADME/potency of the prodrug/drug (e.g., -AZI). The assembled prodrugs would then be named as the combination of these abbreviations, e.g., SS60-CBI-AZI (Figure 2c).

### 2.2. Choice of Modules for Dichalcogenide Prodrugs.

Choosing trigger motifs with the right redox selectivity profile

and cargo release kinetics is key to success of the prodrug design. Our redox trigger choices were based on results from short-term assays relying on phenol-releasing fluorogenic probes (Figure 3). Cyclic 6-membered disulfide (SS60) or

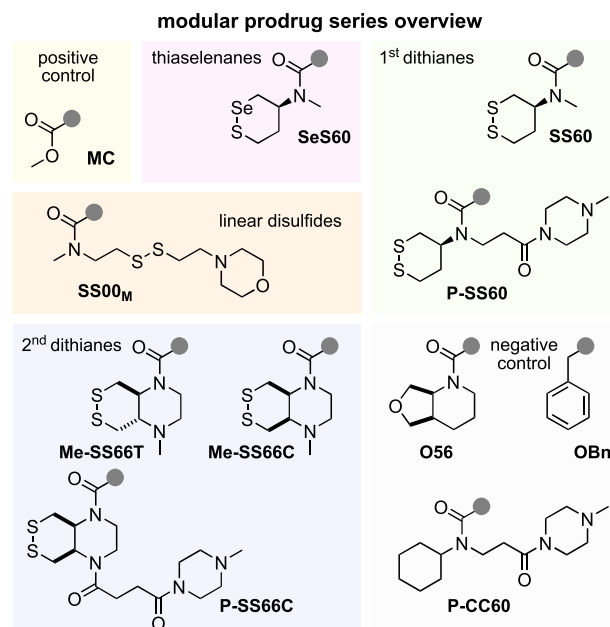


**Figure 3. Redox triggers for modular prodrugs.** 1st generation Trx-triggers SS60 and solubilized P-SS60;<sup>17</sup> 2nd generation solubilized bicyclic Trx-triggers Me-SS66T, Me-SS66C, and P-SS66C;<sup>19</sup> TrxR-trigger SeS60.<sup>18,20</sup> “Upper limit” control triggers: very labile MC, monothiol-labile SS00<sub>M</sub>. “Lower limit” control triggers: hydrolysis benchmarks O56 and P-CC60, and carbamate stability test OBn.

its faster-activated, solubilized analogue (P-SS60) was used as slowly/moderately reduced Trx-selective substrate (minor crosstalk to dithiol Grx is expected<sup>17</sup>). Their unstrained *cis*-annulated-piperazinyl bicyclic congeners (P-SS66C, Me-SS66C) have much faster, though less selective, Trx reductive activation (more crosstalk to dithiol Grx); strained *trans*-annulated congeners (Me-SS66T) are likewise rapidly activated by reductases, but are also moderately labile to monothiols such as GSH, so were expected to produce more unspecifically toxic prodrugs (a more complete view of the cellular selectivity profiles of these dichalcogenides is given in ref 19). Separately from these Trx-targeted triggers, we included the specifically TrxR1-activated cyclic 6-membered selenenyl sulfide SeS60<sup>18</sup> to probe the performance and selectivity possible by targeting the regulator (rather than effector) of the thioredoxin system (Figure 3).

To benchmark the performance of these redox-activated triggers and to separate the contributions of reductive vs non-reductive activation (hydrolytic, oxidative, etc.), we designed “upper limit” and “lower limit” reference triggers. At the extreme end of unspecificity, we used linear disulfides (e.g., SS00<sub>M</sub>) which are unselectively reduced by any biological thiol,<sup>17</sup> as well as a rapidly and unspecifically hydrolyase-cleavable carbonate (MC), to test the potency expected for the fully released drug cargos and so to estimate the degree of release from the hopefully redox-selective triggers. To understand the degree of *non-reductive* drug release which contributes to the prodrugs’ overall cytotoxicity, we would compare the cytotoxicity from a non-reducible isosteric

carbamate (**O56**) or a solubilized analogue (**P-CC60**) to that of a more-resistant ether (**OBn**; Figure 3). An overview of the redox and control triggers is given at Figure S1, where their performance features are detailed.

To complete the prodrugs, we equipped hydroxy-*seco*-CBI with two types of "segment B" indole (Figure 2b). For a benchmark that can be compared to literature results, we used the classic trimethoxyindole **TMI** residue, as found in the original natural products duocarmycin SA/A.<sup>23</sup> The lipophilic **CBI-TMI** tends to aggregate, so this cargo was only employed with the solubilized trigger motifs. To evolve the properties of synthetic duocarmycins, we also designed a novel abiotic segment B, 3-azetidynyl-propoxy-indole (**AZI**), which is the first azetidine used on a duocarmycin. Our hopes were that the basic amine would (i) add solubility so that non-solubilized triggers (e.g., **SS60**, **SeS60**) could be incorporated into useful and bioavailable **AZI** prodrugs and also (ii) increase DNA association by Coulombic interactions, and so raise potency. These two features are known from, e.g., dimethylamine-substituted B segments ("DEI").<sup>29</sup> However, our design also aimed to (iii) avoid undesirable metabolic attack/demethylation *in vivo*, which we expected might be useful for its *in vivo* performance. For an overview of all the resulting prodrug combinations, see the discussion at Figure S3.

**2.3. Prodrug Assembly by a Versatile 2-Step Approach That Avoids Dangerously Toxic Intermediates.** Commercial *O*-benzyl-*N*-Boc-(*S*)-*seco*-CBI (**BnO-CBI-Boc**) **1** served as a synthetic starting point (Figure 4). While

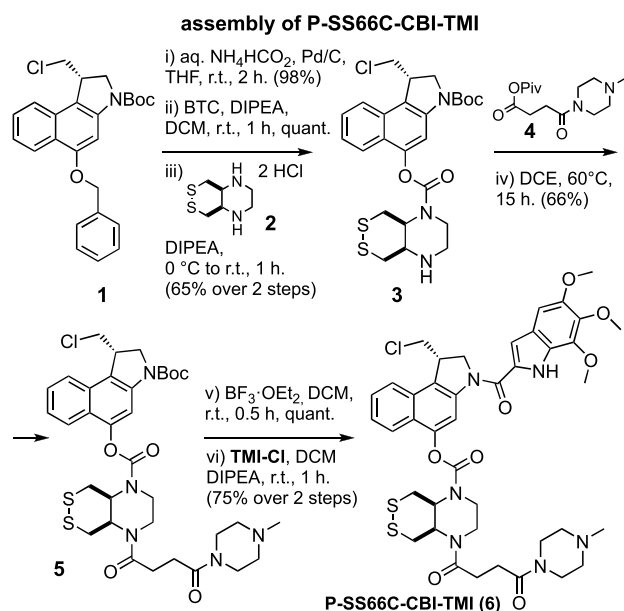


**Figure 4. Modular *seco*-CBI prodrug synthesis.** Synthesis of representative prodrug **P-SS66C-CBI-TMI** from commercial **BnO-CBI-Boc** **1** (full synthesis overview in Figures S2 and S3).

the prodrug retrosynthesis is straightforward, we wished to avoid handling any directly potent DNA alkylators during synthesis; i.e., we aimed to avoid free 5-hydroxy-CBI-indoles that are otherwise the most easily diversified synthetic intermediates, so we wanted to install the triggers before coupling to the indoles. We performed *O*-debenzylation by mild heterogeneous hydrogenation on Pd/C using aq.  $\text{NH}_4\text{HCO}_2$  as the hydrogen source, as reported by Major,<sup>29</sup> to avoid the unwanted naphthalene hydrogenation and

dechlorination seen with  $\text{H}_{2(g)}$ . The phenolic chloroformate produced by reaction with *in situ*-generated phosgene was carbamylated<sup>17,18</sup> with the eight trigger secondary amines, giving good to excellent yields of trigger-CBI intermediates (e.g., trigger **H-SS66C-H** (**2**) giving intermediate **H-SS66C-CBI-Boc** (**3**), Figure 4). The bisamine SS66-type triggers could then be additionally functionalized by reductive amination (e.g., with formaldehyde, giving **Me-SS66-CBI-Boc** species) or acylation (e.g., with acid anhydride **4**,<sup>41</sup> giving **P-SS66-CBI-Boc** species). The indolecarboxylic acid segments had then to be coupled. **TMI-OH** is commercial; we prepared **AZI-OH** by a 4-step literature procedure<sup>42</sup> that we adapted into a 3-step sequence, using Mitsunobu-type *O*-alkylation of a 5-hydroxy-1*H*-indole-2-carboxylic ester with commercial 3-azetidynyl-propan-1-ol.<sup>43</sup> Finally, the trigger-CBI intermediates were *N*-Boc-protected with HCl in organic solutions,<sup>44</sup> with TFA or with  $\text{BF}_3 \cdot \text{OEt}_2$ ,<sup>30</sup> then coupled either to **AZI-OH** with conditions similar to those reported by Tercel<sup>32</sup> or else to the acid chloride **TMI-Cl**,<sup>45</sup> giving the 16 prodrugs and controls used in this study (Figure S3) with moderate overall yields (Figure S2). Note that even traces of residual **CBI-OH**, **CBI\*** cyclopropane, or easily cleaved CBI byproducts must be avoided for cellular and *in vivo* testing; their much higher potency can overpower the true performance of the major species prodrugs.

**2.4. The Prodrugs Are Not Activated by Monothiois, so They May Be Specifically Reducible by Disulfide Reductases in Cells.** The cyclic dichalcogenide redox triggers were previously shown to resist activation by monothiois such as glutathione (GSH) but to allow reduction/cyclization-based release of phenolic fluorophore cargos when treated with disulfide reductase enzymes (e.g., Trx and/or TrxR, Grx, etc.).<sup>17–19</sup> These performance features had not been tested with naphthols, so we used HPLC to test them and show their reduction-based activation sequence (Figure 2c and Figures S4–S6).

In brief, treatment with the quantitative reductant TCEP triggered a reaction cascade matching the activation sequence we expected (Figure 2c): dichalcogenides are reduced to dichalcogenols that cyclize, giving the naphthol cargos (plus thiol trigger byproduct) that evolve to the activated cyclopropanes (Figure 5). Also matching expectations, the redox triggers which previously resisted monothiol-reductant-based release of phenolic cargos (**SS/SeS60** and **SS66C** types) likewise gave no detectable release of 5-hydroxy-*seco*-CBI or cyclopropane **CBI\*** when challenged with 5 mM GSH (50 equiv) over 24 h, though partial activation by GSH was indicated for the strained **SS66T** (Figure S6). The reference compounds performed as expected, either being sensitive to GSH (linear disulfide **SS00<sub>M</sub>**) or else resistant to all reduction conditions (non-chalcogenide **O56** or solubilized **P-CC60**). We also confirmed under the same cell-free conditions that the prodrugs were reductively activated by TrxR and/or Trx, as appropriate (Figure S7).

Taken together, this indicated that the (**P/Me**)-**SS60**, **-SeS60**, and **-SS66C** prodrugs would indeed be monothiol-resistant, giving potential for them to act as prodrugs that are selectively activated by dithiol reductases of the Trx system in cells, and that the reference prodrugs could be used as intended, to estimate the high potency expected if activated by all thiol reductants (**SS00<sub>M</sub>**) or the low potency expected if only activated by non-reductive mechanisms, e.g., hydrolysis (**O56**, **P-CC60**) (Figure 5).

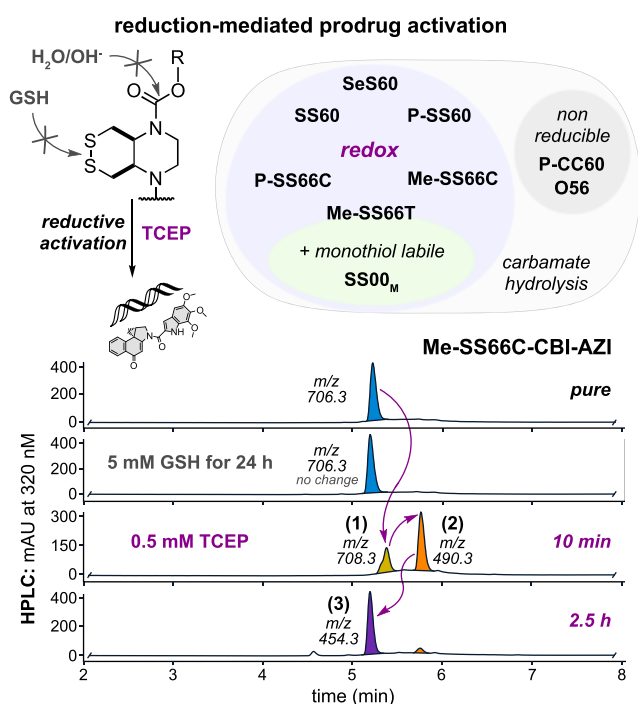


**Figure 5. Reduction-triggered prodrug activation.** HPLC-MS analysis of activation of Me-SS66C-CBI-AZI: (1) TCEP reduction gives the dithiol, (2) the phenolate is expelled, and (3) Winstein cyclization gives the activated cyclopropane (see Figures S4–S6).

**2.5. Tunable Reduction-Based Activity Allows Rational Selection of Reducible Motifs for Future *In Vivo* Applications.** While cell lines vary in their intrinsic sensitivity to duocarmycin drugs, the *relative* toxicity of duocarmycin-type prodrugs, within any single cell type, should reflect their degrees of cellular activation. We were particularly interested in “low-potency” prodrugs, with low activation in usual cell cultures. As a counterexample, prodrugs that are fully activated in all cell types will have high cell culture potencies, like their free duocarmycin cargo, but they are also likely to be activated in all tissues during systemic treatment *in vivo*, so causing dose- and therapy-limiting toxic side-effects.<sup>46,47</sup> Instead, a prodrug that is little activated in most or all 2D cell cultures (lower potency than its free cargo) may escape such broad activation *in vivo* and be well-tolerated, and if it is distributed to tumors with a suitable bioreduction profile, it may be selectively activated there—so delivering therapeutic benefits. Comparing the relative potencies of duocarmycin prodrugs across cell cultures may give valuable indications about their likely tolerance in therapeutic settings.

For example, free CBIs (cellular  $IC_{50}$  ca. 5–30 pM<sup>25</sup>) and hydroxy-*seco*-CBIs (5–50 pM<sup>35,48</sup>) have low tolerated dosages *in vivo*, but their prodrugs are increasingly tolerated, as their cellular activation is reduced from high (esters for esterases: 100–500 pM<sup>27</sup>) to moderate (tertiary carbamates for oxidative and/or peptidolytic processing: 50–300 nM<sup>27</sup>) to low (glycosides for glycosidases: 5–10  $\mu$ M<sup>29</sup>). Amino-*seco*-CBIs are less efficient alkylators than the phenols (100–500 pM<sup>31</sup>); their prodrugs can also be tuned for low non-specific release (nitro prodrugs for metabolic reduction: 5–50  $\mu$ M<sup>32</sup>). Table 1 summarizes these approximate average  $IC_{50}$ s over a range of cell lines, highlighting how duocarmycin prodrug potency can be tuned over ca. 7 orders of magnitude by the choice of bioactivation strategy.<sup>4</sup>

**Table 1. Benchmark Potencies of CBI Prodrug Classes in Cell Culture<sup>a</sup>**

	relative cellular potencies of CBI-based agents			
	literature		this work: redox prodrugs	
	$pIC_{50}$	rel. potency	$pIC_{50}$	rel. potency
activated CBI*	11	100,000	labile carbonate hydrolysis (MC)	9 1,000
HO- <i>seco</i> -CBI	10.7	50,000	unspecific thiol reduction (SS00 <sub>M</sub> )	8 100
H <sub>2</sub> N- <i>seco</i> -CBI	9.7	5,000	TrxR-mediated activation (SeS60)	7.5 30
esters	9.5	3,000	resistant dithianes (SS60/SS66C)	6.5–8 3–100
carbamates	6	1	stable carbamate hydrolysis (P-CC60)	6 1
glycosides	4.3	0.02	stable ether (OBn)	5.5 0.3
nitro-CBIs	4	0.01		

$pIC_{50} = -\log_{10}(IC_{50})$  (M); potencies referenced to carbamate hydrolysis as 1  
literature estimates are geometric averages from different cell lines and compounds

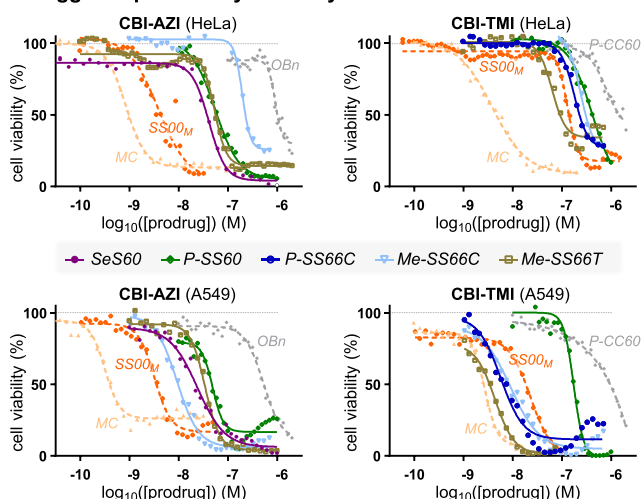
<sup>a</sup>Averaged literature potencies for CBIs and their prodrugs, to put the potencies of the tertiary carbamate redox prodrugs of this work into perspective. Recall that potency maximization within the redox prodrug series is *opposed* to the aim of this work (section 2.5).

We wished to understand the degree of bioreduction-mediated activation across the series of novel dichalcogenide prodrugs by studying their cellular potencies relative to “minimum/maximum-potency” reference compounds. Our redox-activatable prodrugs are tertiary carbamates, which will have some activation by hydrolysis, as well as by bioreduction. We thus expected their cell culture potencies to fall between a minimum for the non-reducible hydrolysis-only carbamates O56 and P-CC60 (ideally: low potency, anticipating low systemic release) and a maximum for the rapidly enzyme-hydrolyzed carbonate MC (bioreductive activation unlikely to be faster than this), within which range variations of potency would report on their relative reductive stability or lability. We also tested non-specifically reducible linear disulfide SS00<sub>M</sub> prodrugs to probe our expectation that only the monothiol-resistant dichalcogenides such as those we recently introduced<sup>17,18</sup> can access a different performance space than prior, linear disulfides.

We used A549 lung cancer and HeLa cervical cancer cell lines for initial screening of the prodrugs. These had a >1000-fold range of potencies: rapidly hydrolyzed MC set an enzymolytic maximum ( $IC_{50}$  ca. 0.5 nM; Figure 6a) that can be approached by linear disulfide SS00<sub>M</sub> (non-specific redox activation by thiols), while the non-reducible carbamates set a hydrolysis-only minimum (ca. 300 nM for O56-CBI-AZI, >1  $\mu$ M for P-CC60-CBI-TMI) that was similar to that of ether OBn-CBI-AZI (>1  $\mu$ M). We thus estimated that the tertiary carbamate design, with its excellent cell culture stability, offers a window of up to 1000-fold toxicity enhancement for the dichalcogenide prodrugs according to how much reductive release they undergo (Figure 6a). (The 3–10 $\times$  higher potency and better reproducibility of our novel, solubilized AZI as compared to TMI series prodrugs are additional positive features.)

The toxicities of the novel cyclic dichalcogenide prodrugs (Figure 6b) revealed increasing redox-based release in the order SS60  $\approx$  SS66C (Trx-activated) < SS66T (Trx-activated plus some monothiol sensitivity) < SeS60 (TrxR-activated with high turnover) < SS00<sub>M</sub> (monothiol-activated limit),

## a trigger-dependent cytotoxicity



**b**

prodrug	IC <sub>50</sub> (nM): HeLa	A549	IC <sub>50</sub> (HeLa)/IC <sub>50</sub> (A549)
<b>CBI-AZI</b>			
1 MC	0.8	1.6	0.5
2 SS00 <sub>M</sub>	6.9	4.1	1.7
3 SeS60	49	60	0.8
4 Me-SS66T	49	51	1.0
5 Me-SS66C	400	12	33
6 SS60	96	120	0.8
7 P-SS60	890	100	8.9
8 O56	460	410	1.1
9 OBn	750	420	1.8
<b>CBI-TMI</b>			
10 MC	4.3	2.9	1.5
11 SS00 <sub>M</sub>	125	35	3.6
12 Me-SS66T	59	5.9	10
13 Me-SS66C	220	17	13
14 P-SS60	420	180	2.3
15 P-SS66C	200	12	17
16 P-CC60	1,250	1,700	0.7

**Figure 6. Trigger-dependent cellular cytotoxicity.** (a, b) Potency in A549/HeLa cells. Note, e.g., consistent 13- to 30-fold greater toxicities in HeLa than in A549 cells for SS66C triggers (AZI or TMI cargos, P- or Me- substituents) (see also Table S1 and Figures S8 and S9).

matching the order in acute assays of their corresponding fluorogenic probes.<sup>17–19</sup> This supports our hypothesis that engineered dichalcogenides can resist non-specific thiol-mediated release even in long-term assays (IC<sub>50</sub>s below SS00<sub>M</sub>). We consider that by avoiding substantial activation in usual cellular conditions (ca. 30–300-fold less release than references MC/SS00<sub>M</sub>), they keep alive the possibility of enhanced release selectively in tumors, as long as their bioreduction sensitivity profile suits the potentially increased expression and/or activity of reductases in tumor environments.

**2.6. Redox Activation Is Tied to Thioredoxin System Activity.** Testing whether the cellular activation of the prodrugs is due to their intended target, thioredoxin, is a non-trivial task: since there are no stable Trx knockouts, nor are pharmacologically clean cellular Trx inhibitors available. A TrxR1 knockout (ko) in mouse embryonic fibroblast (MEF) cells is, however, accessible. We compared its prodrug

sensitivity to that of its parental line<sup>49</sup> (wild-type, wt), on the basis that TrxR1-ko should leave most Trx1 in its oxidized state (only a fraction of it can be maintained in the reduced state by alternative reductants such as Grx2),<sup>50</sup> so prodrugs relying on the cytosolic thioredoxin system (Trx1/TrxR1) for most of their bioreductive activation in long-term assays will have lower potency in TrxR1-ko cells.

The overall MEF potency trends were similar to those in HeLa/A549 cells (pIC<sub>50</sub>: MC > MeSS66T > Me-SS66C ≈ P-SS66C > P-SS60 > P-CC60; Figure 5c and Figure S11). Excitingly, all five prodrugs based on the bicyclic SS66-type trigger, which have the lowest reduction potential of the disulfide series, were many-fold less potent against TrxR1-ko than wt cells (Figure 7). This is consistent with reductive

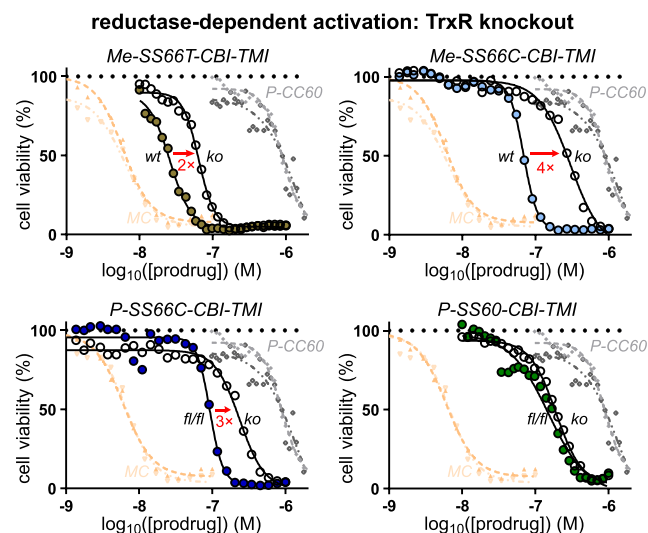


**Figure 7. Target-dependent cellular cytotoxicity.** Comparing prodrug toxicities in intact (wt) vs TrxR1-knockout (ko) MEF cells to test whether the major cellular activation route is rate-limited by the cytosolic thioredoxin couple (TrxR1/Trx1). That is indicated for bicyclic -SS66C and -SS66T but not monocyclic -SS60 (see also Table S1 and Figure S10).

processing of SS66 strongly requiring thioredoxin system activity. That is not an obvious result since the multi-day assay provides plenty of time for dithiol reductases outside the TrxR1/Trx1 system (e.g., Grxs) to perform reductive activation instead. Indeed, the three less-stabilized monocyclic SS60-type prodrugs showed no such fold-change of potency (see Table S1 and Figure S10), suggesting that, in long-term assays, cellular activation of simple dithianes can proceed through multiple redox paths. We also find it satisfying that there is such a clear division between the SS66 and SS60 structural classes. No matter which cargo (AZI or TMI) and what variable substituents (P- or Me- type) are employed, it is the core chemical nature of the redox trigger that dictates cellular performance. Although some redox papers have resisted the idea that structure–reactivity relationship (SAR) rules operate for reducible probes,<sup>16</sup> just as they do for drugs, we believe that such consistent patterns will continue to emerge and to enlighten the field, wherever design and testing are performed comprehensively.

Taken together, these assays had validated the hypothesis of tunable redox-based cellular activation of dichalcogenide prodrugs. Consistent with our aims, the SS66-type strongly depend on a specific, key enzyme pair, the thioredoxin system,

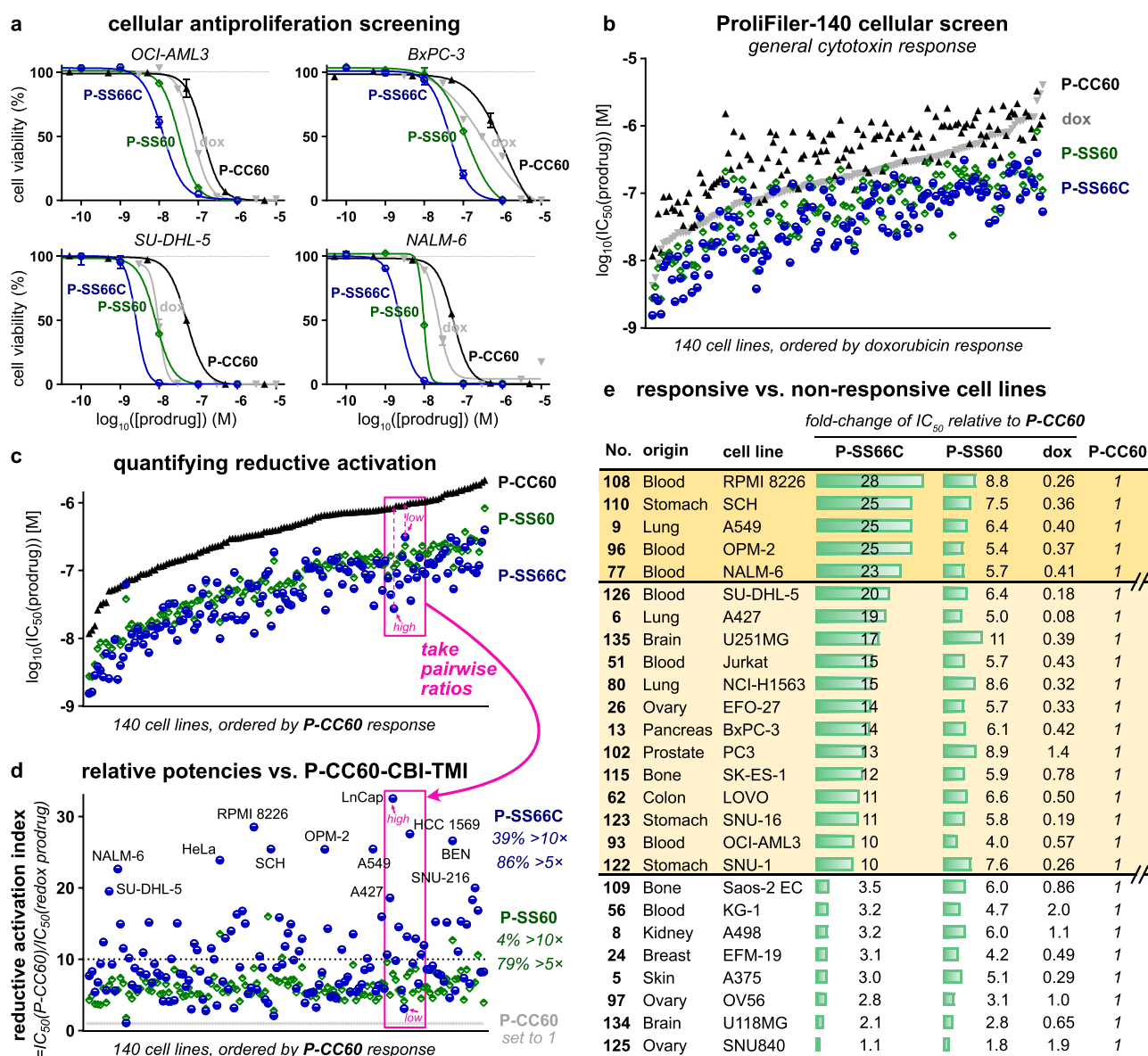


**Figure 8.** Screening bioreductive activity patterns for P-SS66C-CBI-TMI and P-SS60-CBI-TMI redox prodrugs by benchmarking against hydrolysis control P-CC60-CBI-TMI, across 140 cancer cell lines (“Prolifer-140”). (a) Sample cell lines of the 140 tested (see too Table S2 and Figures S11 and S12). (b) Rank ordering by sensitivity to the mechanistically unrelated drug doxorubicin. (c) Rank ordering by sensitivity to hydrolysis control P-CC60. (d)  $IC_{50}$ s as ratios relative to that of P-CC60 hydrolysis control. (e) Sets of cell lines suggest different redox activity patterns.

even in long-term assays (Figure 7). This validates the first bioreductive prodrug design capable of selectively targeting a disulfide reductase in cells.

**2.7. Profiling Thioredoxin- and Redox-Activated Prodrugs in 176 Cancer Cell Lines Suggests Their *In Vivo* Potential.** We wished to study the *in vivo* suitability of the dichalcogenide strategies while benchmarking the performance of the different triggers in a thorough and reproducible manner that can be used to guide rational future design of other prodrug families. We therefore planned to screen the prodrugs’ redox-dependent bioactivity across large numbers of validated cancer cell lines with standard and objective assay conditions.

We initially focused on P-SS66C (reducible by thioredoxin) and P-SS60 (reducible by thioredoxin and unknown other actors). Both will also undergo non-reductive release by

carbamate cleavage (hydrolases and/or oxidative metabolism) at rates that are likely to vary with cell type. Other factors depending on cell type include intrinsic cellular sensitivity to the duocarmycin cargo and cell entry rate and degree of accumulation of the prodrug. To control for all these cell-line-dependent features, we included the closely similar but non-reducible carbamate analogue, P-CC60. We think this is a vitally important step. Rather than focusing on the absolute potencies of a redox prodrug in a certain cell line, we could then examine the fold difference of potency between reducible P-SS66C or P-SS60 vs non-reducible P-CC60, to focus on the degree of bioreductive processing that the prodrugs undergo in cell culture (see below).

Note that while expression of some reductases has been measured on mRNA and protein levels, their actual activity levels are unknown in clinically relevant samples (e.g., patient

tumors) as well as simple cell lines, due to the lack of suitable tools to quantify them. Thus, we were also interested to explore if expression patterns might or might not correlate to drug potency profiles (see below).

We obtained a first high-throughput automated screen of the antiproliferative potencies of reducible **P-SS66C-CBI-TMI** and **P-SS60-CBI-TMI** alongside **P-CC60-CBI-TMI** as a hydrolysis-only reference over a panel of 140 standard cancer cell lines with diverse tissue origins (skin, ovary, lung, colon, breast, pancreas, prostate, kidney, brain, etc.), run by commercial provider Reaction Biology (“Prolifer-140” screen). The topoisomerase inhibitor doxorubicin served as a benchmark for assay validation and to illustrate trends in cell line drug sensitivity. Incubations were performed for 72 h before automated viability readout with CellTiterGlo (Figure 8).

All 140 cell lines gave well-formed and complete sigmoidal dose–response curves with steep and uniform Hill slopes, consistent with excellent assay technical performance, including compounds being well soluble at all concentrations (selection in Figure 8a, full data in Table S2 and Figure S11). Antiproliferative  $IC_{50}$  values range from ca. 1 to 100 nM for reducible **P-SS60** and **P-SS66C** and from ca. 10 to 1000 nM for non-reducible **P-CC60** (Figure 8b). Prodrug potencies correlated slightly to those of doxorubicin (Figure 8b) but much better to **P-CC60** (Figure 8c), matching expectations from their overall similar structures and shared mechanism of action. Notably, **P-SS60**'s potency correlated more tightly than **P-SS66C** to that of **P-CC60** (green vs blue data, Figure 8c). This difference now gave broad support to the indication from the single cell line TrxR knockout assay (Figure 7) that their bioreductive activating mechanisms in long-term assays are substantially differentiated.

Matching our model, the potencies of reducible **P-SS60** and **P-SS66C** were greater than those of non-reducible **P-CC60** within each one of the 140 cell lines, even though their absolute potencies vary over more than 100-fold between the different cell lines. This supports **P-CC60** being a suitable predictor of minimal, purely non-reductive release levels in any given cell line—compared to which, any additional reductive release is reflected in increased potency of the reducible prodrugs (Figure 8a,c).

This additional reductive release is, in our opinion, the most important data delivered by the screening. To analyze it, we define a prodrug's “reductive activation index” in a given cell line to reflect how many fold more potent it is than the hydrolytic control: i.e.,  $index = IC_{50}(P-CC60)/IC_{50}(prodrug)$  (Figure 8d). This is a qualitative indicator of how much reductive activation a prodrug experiences, benchmarked to an unknown but variable level of hydrolytic cleavage, in a given cell line.

Trends emerge when the reductive index is viewed across so many cell lines (selection in Figure 8e, full list in Table S2): (1) The index of **P-SS66C** is variable, with some cell lines reaching up to 30-fold, and there is no relation between which cell lines have a high index and which are most sensitive to **P-SS66C** in an absolute sense (Figure 8d). This contrasts to **P-SS60**, whose index remains in a narrow band between 5 and 8 over nearly all cell types. Figure 7 had indicated that TrxR1 activity strongly impacts the bioreductive activation of **P-SS66C** but not of **P-SS60**. Thus, it is tempting to interpret the index of **P-SS66C** as reporting substantially on variations of specific TrxR1 activity and to see the index of **P-SS60** as

reporting on other bioreductive actors which seem more constant. (2) The cell lines can be grouped by suggestive trends in the reductive index. For example: (i) *high index for P-SS66C but not P-SS60* (Figure 8e, top bracket), suggesting cell lines where comparatively high reductive activity driven by TrxR1 could be harnessed with novel bioreductive prodrug strategies such as the modular Trx/TrxR-dichalcogenides we present; (ii) *index for P-SS60 is similar to that of P-SS66C* (Figure 8e, middle bracket), suggesting significant disulfide bioreduction activity outside the Trx1/TrxR1 couple that may be exploitable by future prodrugs tuned toward other reductases, e.g., Grxs; or (iii) *low indices for both redox prodrugs* (Figure 8e, bottom bracket), where bioreduction is outweighed by other cleavage mechanisms, so dichalcogenide prodrugs may be unsuitable for addressing these cell types.

We also used this large dataset to check for biological features that might correlate usefully to reductive activation. First, we tested whether reductive performance was clustered according to the tissue of origin of the cell lines, which could be suggestive of, e.g., cancer indications that might be promising for selective targeting by reductive prodrugs. However, the tissue of origin played no role in either the reductive index or the absolute potency of the compounds tested (Figure S12). Second, we wished to examine if prodrug potency correlated to gene transcript levels, which could have suggested biomarkers predictive for response to redox prodrugs, thus orienting their therapeutic opportunities. However, mRNA transcript analysis did not give confidently interpretable results, and we believe that direct (e.g., fluorogenic) protein activity probes would be better prodrug predictors (see Table S2).

We next wished to test the reproducibility and validity of these results by standardized screening in a different lab and location, while scrutinizing in more detail the bicyclic **SS66** structure which had indicated tantalizing TrxR/Trx selectivity. We obtained a second high-throughput automated screen of antiproliferative potencies through the non-commercial NCI Developmental Therapeutics Program (DTP) over the NCI-60 standardized human tumor cell line panel.<sup>51</sup> 19 of the NCI cell lines overlap with the Prolifer-140 screen, so they could be used for benchmarking TMI results, although differences in assay setup, run time, and readout will introduce systematic shifts in absolute potencies. For both TMI and AZI prodrug series, we newly tested bicyclic **Me-SS66C** and its more easily reduced diastereomer **Me-SS66T** (basic amines at the redox site) against linear **SS00<sub>M</sub>** and previously tested monocyclic **P-SS60**. We also tested **P-SS66C** and non-reducible **P-CC60** in the TMI series and non-reducible ether **OBn** in the AZI series (Figure 3).

The new prodrugs showed dramatically how stereochemistry and topology determine compound release even in long-term cell assays. *trans*-dithiane **Me-SS66T** was consistently far more potent than any other prodrug, with a mean reductive index ca. 70, while *cis*-dithiane **Me-SS66C** was roughly similar in potency to **P-SS60**, with a mean index ca. 7 (selected TMI series in Figure 9a, full TMI and AZI in Figure S13 and Table S3). Also matching expectations from cell-free biochemistry, the reductive index of the monothiol-reducible linear prodrug was far higher than that of its monocyclic or **SS66C** bicyclic analogues. These consistent results highlight that the redox prodrugs' performance and reductive index are fixed by its redox trigger chemistry (pairwise comparisons in Figure S13).



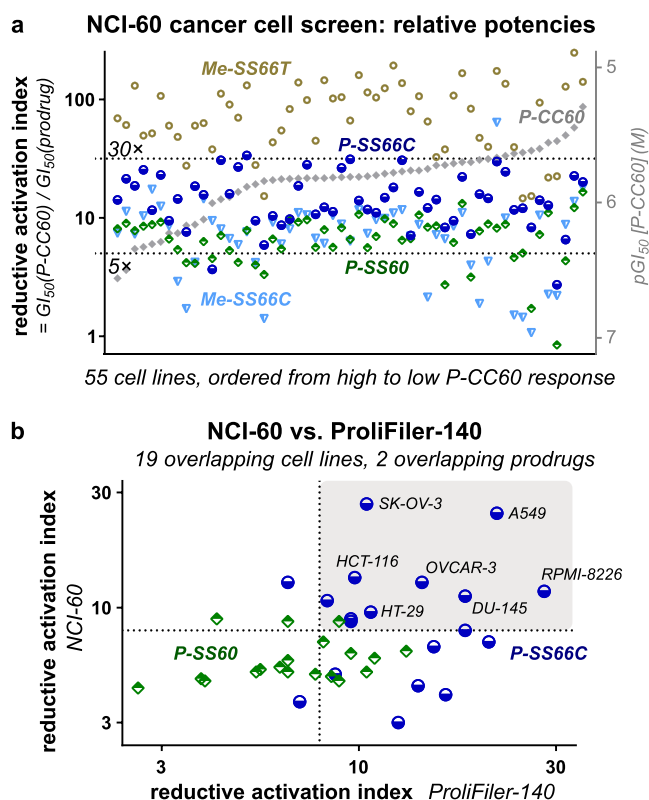


**Figure 9.** Independent bioreductive activity screens across the standard “NCI-60” panel. (a) Selected NCI results for TMI prodrugs (full data in Figure S13 and Table S3a,b). (b) NCI-60 and Proliferator screens give similar TMI series reductive activation (see Table S4).

The benchmarking results of the reductive index also matched well between NCI and Proliferator screens: e.g., (1) variable P-SS66C index (average 14, maximum 30), but with nearly all P-SS60 index in a narrow range around 6–8 (Figure 9a), and (2) no trends from the cell lines’ tissue of origin (Table S3a). As expected, the absolute potencies of a prodrug in a given cell line differed between the screens (Proliferator: average 4-fold higher, standard deviation 3.2-fold). Pleasingly though, despite these differences, the reductive index was well conserved between the screens (Figure 9b), particularly for P-SS66C (average 1.8-fold higher, standard deviation 1.1-fold) (Table S4). This suggests that the index reports reproducible aspects of reductive release, which in turn supports that the results of these screens (NCI-60: tested more prodrugs, Proliferator: tested more cell lines) can be combined, building an unprecedented, predictive, modular overview of trigger- and cell line-dependent bioreductive performance for novel dichalcogenide bioreductive prodrugs.

We again took advantage of the large screening data to test for potential correlations between drug potency and easily measurable biomarkers, here, proteomics-based protein expression levels. Neither absolute potencies nor the reductive indices were well correlated to the expression of any specific reductases (including Trx1, TrxR1, etc.; Figure S14). Considering the many layers of post-translational regulation of redox activity, we find this unsurprising. We argue further that such a lack of mRNA and protein level correlations probably highlights a need for the redox field to avoid considering gene/protein expression levels as suitable data to propose pathological mechanisms or therapeutic opportuni-

ties—these may be better argued by analyzing activity (note Figure S14).

Taken together, these first-ever high-throughput screens for reductase-targeting disulfide prodrugs showed outstanding performance features. Referencing analysis to the key hydrolytic control factors out variable aspects of cell entry, non-reductive prodrug activation, and intrinsic cell line sensitivity, to show how redox SAR robustly predicts prodrug performance in these long-term assays, across 176 cell lines from many tissue types of origin. The reductive activation indices are reproducible in different laboratories and setups, they follow clear trends across cell lines, and above all they match the molecular understanding gained from simple cell-free and cellular assays<sup>17</sup> of how the trigger structures (*trans*- or *cis*-fused, monocyclic or bicyclic) influence acute kinetic lability and reductase promiscuity. The modular tertiary carbamate design is crucial for reaching this intercomparability of results and combines with the choice of the unmaskable, irreversibly DNA-alkylating CBI as cargo to ensure that robust and reproducible data quality can be obtained by machine screens. This sets solid foundations for rational design or selection, and stringent validation, of reducible dichalcogenides as redox prodrug triggers in future work, even on vastly different cargos, which has been one goal of our methodological research.

The second goal of these screens was to test if any reducible triggers generally displayed the moderately activation-resisting performance that we sought for systemically well-tolerated prodrugs, with potential for stronger tumoral bioreductive activation toward anticancer use *in vivo*. Me-SS66C, P-SS60, and P-SS66C appeared suitable for this (indices usually ca. 5–20).

It is important to clarify that, although this screening identified some cancer cell lines with low nanomolar sensitivity to duocarmycin prodrugs in general (e.g., SK-MEL-28), this study did not aim to perform therapeutic assays by implanting such cargo-sensitive cell lines *in vivo*. In our opinion, such assays do not deliver useful information, since they are biased to “succeed” in a way that is not replicable in uncontrolled clinical settings (cf. section 2.9). By focusing instead on the properties conferred by the triggers, we hoped to identify modular motifs that would be generally tolerated for high repeated dose administration, no matter the cargo. We therefore moved on to test these prodrugs *in vivo* in mice.

**2.8. *In Vivo* Pharmacokinetics and Prodrug Tolerance.** We first examined the *in vivo* pharmacokinetics of representative compound SS60-CBI-AZI in Balb/c mice after i.v. administration at 5 mg/kg (3 animals per time point, 4 time points from 5 to 90 min post injection). Compound plasma half-life was ca. 20 min by HPLC-MS/MS (Figure S15a). Matching expectations for a low-release prodrug, no released HO-CBI-AZI, or activated cyclopropane, or adducts, were detected. This gave confidence that the redox prodrugs might give low systemic exposure of the activated CBI and therefore be tolerable *in vivo*.

To test if low prodrug activation could enable *in vivo* use, we performed dosing and toxicity studies in Balb/c mice, comparing the toxicity and the tolerated dosing of low-reducible SS60-CBI-AZI or substantially reducible SeS60-CBI-AZI and to those of non-reducible carbamate OS6-CBI-AZI. Single-dose toxicity was studied over the range 0.1–10 mg/kg. Dosing at  $\leq 3$  mg/kg was typically tolerated, which should be compared to the toxicity limit for fully activatable duocarmycins: typically ca. 0.1 mg/kg for total, cumulative

dose.<sup>46</sup> However, 10 mg/kg of any AZI carbamate was lethal in the week following treatment, though the ether control was not lethal at this dose and not even body weight variations were noted for it, suggesting that, at this dose, even hydrolytic carbamate release passes the threshold for toxicity.

The potential for toxicity under low repeated dosing was then studied, comparing SS60- and SeS60- to O56-CBI-AZI (injections once per week over 3 weeks; 7 animals per condition) (Table 2). No adverse body weight losses were

**Table 2. Tolerability for Repeated Dose Administration *In Vivo* (Mouse)<sup>a</sup>**

prodrug	studies	dose (mg/kg)	remarks
SS60-CBI-AZI	PK, MTD	0.3–1	adverse effects
SeS60-CBI-AZI	MTD	0.3–1	adverse effects
O56-CBI-AZI	MTD	1	
P-SS60-CBI-AZI	MTD, efficacy	3	well tolerated
P-SS60-CBI-TMI	MTD, efficacy	3	well tolerated
P-SS66C-CBI-TMI	MTD, efficacy	3	well tolerated
Me-SS66C-CBI-TMI	MTD, efficacy	3	well tolerated
Me-SS66T-CBI-TMI	MTD, efficacy	3	well tolerated
P-CC60-CBI-TMI	MTD, efficacy	3	well tolerated

<sup>a</sup>The table summarizes dosages that are well-tolerated under weekly or twice-weekly administration, as tested in multiple study settings (PK: pharmacokinetics; MTD: maximum tolerated dose).

seen, but two toxicity features were identified. First, liver damage was indicated by statistically significant, ca. 10% increases of liver weight for the reducible probes, often with increased alanine aminotransferase levels and decreased alkaline phosphatase levels (liver damage markers); these changes were much lower for hydrolytic O56. Second, anemia was indicated by statistically significant decreases of typically 4–12% in hemoglobin, hematocrit, and red blood cell count for all CBIs (Figure S15b). All other organ weights and gross pathology features were normal. Given the small statistical power of the assay, these results should be taken cautiously, but they are consistent with the liver as a site of primarily reductive activation of the monocyclic dichalcogenides.

Next, a moderate repeated dosing study in Balb/c mice (3 animals per group) tested the importance of solubilizing the prodrugs. For example, we have seen elsewhere that a solubilizing piperazinamide P- side chain near the dichalcogenide greatly increases the reproducibility of cellular results.<sup>18</sup> Now, *in vivo*, P-SS60-CBI-TMI was tolerated at once weekly 3 mg/kg dosing in all animals over 3 injections, without adverse effects at the end of observation 2 weeks later. By contrast, at 3 mg/kg, the still monobasic but less soluble analogues SS60-CBI-AZI and SeS60-CBI-AZI led to significant loss of body weight (Figure S15c) with visible adverse effects at the injection site, potentially arising from local aggregation or precipitation since they were avoided by lower dosing at, e.g., 1 mg/kg. This suggested solubilization near the reducible trigger could indeed be beneficial for tolerability.

A larger study was run in 50 athymic nu/nu NMRI mice (10 animals per group) inoculated with BxPC-3 pancreatic cancer cells since the study had been intended as a therapeutic efficacy trial (see section 2.9). Similarly solubilized SS66C derivatives were now included. In this study, the tumor growth rates in all animals were much lower than in any previous or subsequent trials (Figure S16c), so we could only extract data about drug tolerability, not antitumor efficacy. Still, the study confirmed

that the solubilized P-SS60-, Me-SS66C-, and P-SS66C-prodrugs of -CBI-TMI, and the corresponding carbamate hydrolysis control P-CC60-CBI-TMI, were tolerated with twice weekly injections at 3 mg/kg, over a course of five injections, in all animals, since no distinct differences of body weight or animal health were seen as compared to the vehicle control (Figure S16a).

Finally, another large study intended for antitumor efficacy also had to be examined only in terms of tolerability. This assay in immunocompetent Balb/c mice (10 animals per group), inoculated with 4T1 murine breast cancer cells, also treated animals with reducible P-SS60-, Me-SS66C-, or P-SS66C-CBI-TMI or carbamate control P-CC60-CBI-TMI (3 mg/kg) once or twice per week. Here, tumors grew well in all groups, but since even the technical positive control irinotecan failed to slow tumor growth (Figure S16d), no efficacy conclusions could be drawn. Repeated dosing at 3 mg/kg was, however, tolerated also in this mouse strain, again in mice bearing the additional burden of tumors (Figure S16b). This excellent tolerability supported our aim to develop solubilized, low-release, reducible carbamate prodrugs for *in vivo* use with duocarmycin-type cargos.

**2.9. Dichalcogenide CBI Prodrugs Show Anticancer Efficacy in Murine Cancer Models.** We then moved to *in vivo* anticancer efficacy trials of these prodrugs. We anticipated that the *in vivo* growth environments significantly regulate the tumoral redox/metabolic biochemistries which can activate the prodrugs, so we did not expect cell lines' reductive indices from 2D cell culture to be reproduced *in vivo*, but instead we selected tumor models for their technical reproducibility and for their value as biologically meaningful or medically relevant models (Figure 10a). As one model we chose the syngeneic murine breast cancer 4T1, implanted orthotopically (at the native tissue site) into the fat pad of immunocompetent Balb/c mice (i.e., offering a realistic immune system and tumor microenvironment). This model gives rapid, aggressive tumor growth.<sup>52</sup> As a second model, we chose to xenograft human BxPC-3 pancreatic adenocarcinoma cells into immunodeficient hosts. This is a slower-growing model, with low metastasis, that can be more resistant to traditional antimitotic therapy.<sup>53,54</sup> Mice were implanted, randomized once tumors reached 100–150 mm<sup>3</sup> volume, and treated once or twice weekly with prodrug or control compounds typically at 3 mg/kg (8–12 animals per condition, Figure 10a). Tumors were measured by caliper during the assay and weighed at termination.

The 4T1 efficacy study compared reducible P-SS60-CBI-TMI to non-reducible P-CC60-CBI-TMI (3 mg/kg). This time, the technical positive control irinotecan showed the expected tumor-slowing effect. Both reducible prodrugs and non-reducible control delayed tumor growth in the first week of treatment. However, only the reducible prodrugs maintained statistically significant tumor suppression until study termination (Figure 10b,d and Figure S17). Although other interpretations are possible, this is highly suggestive that reductive activation in tumors indeed delivers CBI at effective tumor-suppressing levels that are also significantly above those provided by systemic or tumoral carbamate hydrolysis.

Finally, we tested P-SS60-CBI-TMI in the slower-growing pancreatic cancer model BxPC-3 in athymic NMRI mice (8 animals per group). The response to once-weekly P-SS60 treatment (3 mg/kg) was outstanding: almost identical tumor suppression as the technical control irinotecan (10 mg/kg), with consistent ca. 70% tumor growth rate suppression over 4

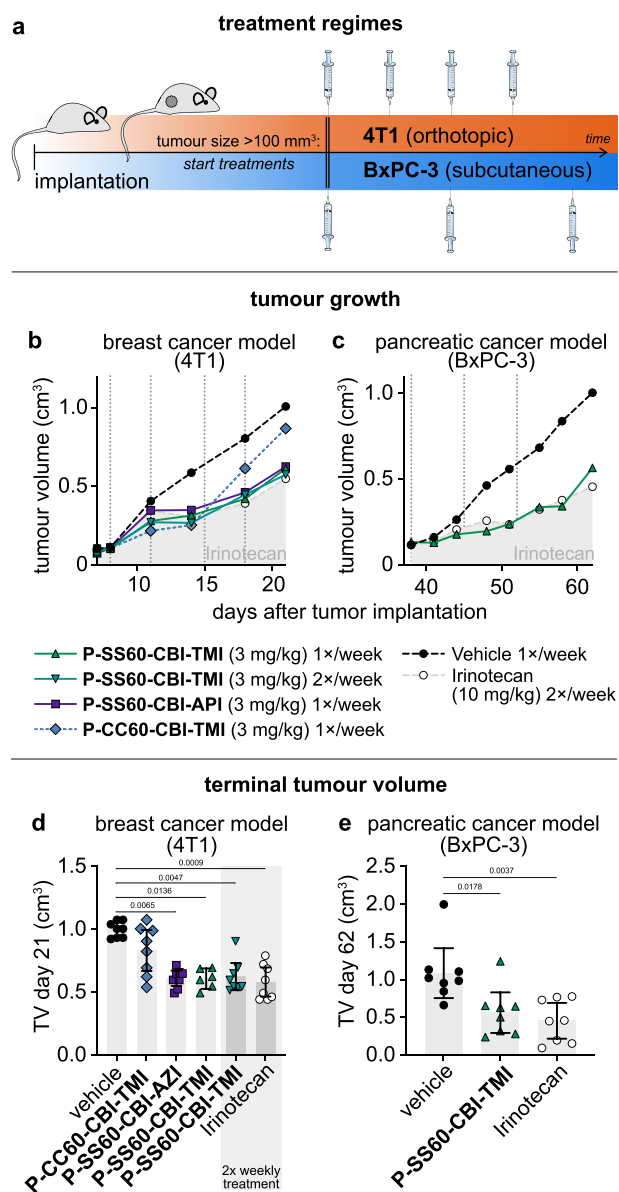


**Figure 10.** *In vivo* anticancer efficacy. (a) Designs for mouse anticancer efficacy assays: murine breast cancer (4T1) implanted orthotopically in the mammary fat pad of immunocompetent Balb/c mice and human pancreatic cancer (BxPC-3) implanted subcutaneously in athymic nu/nu NMR1 mice. (b, c) Tumor volume (TV) over the course of the studies (median values). (d, e) TV at study termination (raw values with means; days 21 and 62, respectively; *p*-values from Kruskal–Wallis test indicated where *p* < 0.05). See also Figure S17.

weeks and high statistical significance (Figure 10c,e and Figure S17). As the P-CC60 non-reductive control had not been included, we cannot estimate how much of the therapeutically beneficial effect in this model stems from reductive or non-reductive CBI release, but at least in cell culture, BxPC-3 had reductive release 6-fold higher than the non-reductive level alone (Figure 8e), so we expect that, similarly, tumoral reductive release may be a significant factor.

After these promising studies showing efficacy and supporting the importance of reductive release, the critical question is now: Is reductive CBI release higher in tumors than in healthy tissues? This cannot be answered from efficacy data alone, since acute tumoral response to CBI is different from

that of healthy tissues, and exposure to released CBI cargo is also challenging to track in tissue by typical HPLC methods, due to its low ( $\sim$ sub-nanomolar) levels that irreversibly alkylate DNA. To tackle this question and thus to estimate the potential of these dichalcogenide strategies to provide tumor-selective drug delivery, we have now begun a new *in vivo* assay program with a different set of bioreductive prodrugs that allow sensitive tracking and quantification of release. Results will be reported in due course.

### 3. SUMMARY AND CONCLUSIONS

We have developed a novel, modular chemical space of bioreductive dichalcogenide prodrugs for the as-yet unaddressed target space of disulfide reductases such as the thioredoxin system (Figure 1). The 10 redox-sensitive triggers and controls allowed us to resolve contributions of reductive vs non-reductive prodrug activation, and the 16 prodrugs (including a novel CBI azetidine) allowed us to test a modular “redox SAR”-based design hypothesis, relying on minimal and maximal activation controls (Figures 2–4). We have confirmed their reductive activation mechanisms (Figure 5) and used cellular knockout assays to quantify triggers that can reach up to  $\geq 80\%$  cellular selectivity for activation by the thioredoxin system (Figures 6 and 7). Two independent, automated, high-throughput cellular screens in 176 cancer cell lines confirmed the redox SAR principle of rationally tuned prodrug potency; they deliver an unprecedentedly comprehensive body of data which we argue indicates actual disulfide reductase activity, as distinct from reductase gene expression or protein levels, across this broad range of cell types (Figures 8 and 9). Several of the solubilized prodrugs were well tolerated *in vivo* over multiple trials, supporting their design principle of high metabolic and hydrolytic robustness, which we believe is a prerequisite for effective tumor-selective reductive release. Tolerability is a stringent hurdle for duocarmycin prodrugs, due to their severe, cumulative toxicity, so this success is encouraging for future applications (Table 2).

Most importantly, *all these aspects*, from synthesis to systemic robustness *in vivo*, are modular features of the dichalcogenide prodrug strategy, so the same principles and performance can be expected from *any* cargo that is used with this (stabilized dichalcogenide plus tertiary carbamate) prodrug approach.

By combining tolerability with efficacy, this first set of CBI prodrugs also indicates that using the dichalcogenide prodrug strategy (even with the historically difficult-to-tame CBI cargo) can be a promising route for *in vivo* anticancer applications. In particular, piperazinamide P-SS60-CBI-TMI gave high anti-tumor efficacy in the relatively resistant BxPC-3 pancreatic cancer model, on the same level as a 3-fold higher dose of FDA-approved irinotecan, and it likewise gave good efficacy in the aggressive syngeneic 4T1 breast cancer model (Figure 10).

More broadly, we expect that, while the tolerability is a general feature of the redox prodrug platform which can benefit any chemical cargo or animal model, efficacy within the tolerability window will only be reliably achieved by matching the choices of model, redox trigger, and cargo type. This multi-variable problem requires a much deeper knowledge level around disulfide manifold bioreduction than currently available. However, by separating the features of prodrug performance that are based on redox reactivity of the trigger from those that are based on trigger hydrolysis, as well as separating the model-dependent and cargo-dependent con-

tributions to results, the systematic modular approach we present makes significant advances toward reaching this level.

The ideal goal for redox prodrugs is to develop a platform approach that can maximize the ratio of drug exposure in tumoral vs healthy tissues, rather than relying only on differences of their intrinsic sensitivities to a given cargo. Testing this exposure ratio with directly quantifiable redox reporter prodrugs based around another cargo besides the CBIs is our aim in ongoing work.

Quantifying exposure with reporters, and developing increasingly effective prodrug-based therapeutics, are mutually reinforcing advances for testing the potential of bioreductive prodrugs. We believe that both will be required, over multiple interleaved cycles of refinement, in order to face this multi-variable problem with a quantitative, SAR-based understanding. We anticipate that the systematic body of predictive data in this study, which complements previous *in vitro* development steps,<sup>16–19</sup> should prove vital to enable and orient such *in vivo* follow-up cycles, and we believe that direct reporter methods will at last start to reveal the selectivity that engineered, synthetic dichalcogenide redox substrates can deliver by harnessing oxidoreductase-based release in the disulfide/dithiol manifold.

That challenge should not be underestimated: bioreductive release prodrug systems based on oxidized nitrogen species have taken several *decades* to reach their current, and still incomplete, level of predictive or SAR-based understanding.<sup>3,32</sup> However, we believe that, by emphasizing a high volume of comparative SAR-based data, this work will help quantitative *in vivo* investigations to succeed rather more rapidly.

A reliable, actionable understanding of the disease indications in which redox dysregulation can be exploited, and to what degree it may provide selective therapeutic benefits, would resolve several decades of tantalizing observations and theoretical deadlock. These dichalcogenides are bringing a new biochemical target space into play: time will tell if they can be used as straightforwardly as in this study, i.e., modularly retrofitting existing cargos to turn them into powerful bioreductive diagnostics and prodrugs.

## ■ ASSOCIATED CONTENT

### SI Supporting Information

The Supporting Information is available free of charge at <https://pubs.acs.org/doi/10.1021/acscentsci.2c01465>.

Synthesis, analysis, biochemistry, cell biology, and *in vivo* biology, including Figures S1–S17 and Tables S1–S5 (PDF)

Prodrug potency screening and reductive index data across 176 cell lines, and test gene expression correlation data, in accessible format for further analysis (XLSX)

Transparent Peer Review report available (PDF)

### Accession Codes

The Accession Code CCDC 2214471 contains the supplementary crystallographic data for this paper. These data can be obtained at [www.ccdc.cam.ac.uk](http://www.ccdc.cam.ac.uk).

## ■ AUTHOR INFORMATION

### Corresponding Author

Oliver Thorn-Seshold – Department of Pharmacy, Ludwig-Maximilians University Munich, 81377 Munich, Germany; [orcid.org/0000-0003-3981-651X](https://orcid.org/0000-0003-3981-651X); Email: [oliver.thorn-seshold@cup.lmu.de](mailto:oliver.thorn-seshold@cup.lmu.de)

## Authors

Jan G. Felber – Department of Pharmacy, Ludwig-Maximilians University Munich, 81377 Munich, Germany; [orcid.org/0000-0002-5010-9624](https://orcid.org/0000-0002-5010-9624)

Annabel Kitowski – Department of Pharmacy, Ludwig-Maximilians University Munich, 81377 Munich, Germany

Lukas Zeisel – Department of Pharmacy, Ludwig-Maximilians University Munich, 81377 Munich, Germany; [orcid.org/0000-0001-7813-7099](https://orcid.org/0000-0001-7813-7099)

Martin S. Maier – Department of Pharmacy, Ludwig-Maximilians University Munich, 81377 Munich, Germany; [orcid.org/0000-0002-0409-0539](https://orcid.org/0000-0002-0409-0539)

Constanze Heise – Department of Pharmacy, Ludwig-Maximilians University Munich, 81377 Munich, Germany

Julia Thorn-Seshold – Department of Pharmacy, Ludwig-Maximilians University Munich, 81377 Munich, Germany; [orcid.org/0000-0002-4879-4159](https://orcid.org/0000-0002-4879-4159)

Complete contact information is available at:

<https://pubs.acs.org/10.1021/acscentsci.2c01465>

## Author Contributions

J.G.F. performed synthesis, analysis, cell-free prodrug activation and cellular assays, coordinated screening, analyzed screening data and performed data assembly. A.K. performed cell-free prodrug activation and cellular assays, coordinated screening and *in vivo* studies, and performed data analysis. L.Z. and M.S.M. performed synthesis and analysis. C.H. performed cell-free prodrug activation and cellular assays. J.T.-S. designed, coordinated, and analyzed *in vivo* studies and performed data assembly. O.T.-S. designed the concept and experiments, supervised experiments, performed screening data analysis and coordinated data assembly. J.G.F. and O.T.-S. wrote the manuscript with input from all authors.

## Funding

This research was supported by funds from the German Research Foundation (DFG: SFB 1032 project B09 number 201269156, SFB TRR 152 project P24 number 239283807, SPP 1926 project number 426018126, and Emmy Noether grant 400324123 to O.T.-S.); LMUExcellent (Junior Researcher Fund to O.T.-S.); the Munich Centre for Nano-Science initiative (CeNS to O.T.-S.); and Federal Ministry of Education and Research GO-Bio 161B0632 to O.T.-S. and J.T.-S..

## Notes

The authors declare the following competing financial interest(s): J.G.F., L.Z., J.T.-S. and O.T.-S. are inventors on patent applications PCT/EP2022/057483 and PCT/EP2022/059280 filed by the Ludwig-Maximilians-University (LMU) Munich in 2021, covering compound structures reported in this paper.

## ■ ACKNOWLEDGMENTS

J.G.F. thanks the Studienstiftung des Deutschen Volkes for support through a Ph.D. scholarship; L.Z. thanks the Fonds der Chemischen Industrie (FCI) for support through a Ph.D. scholarship; J.T.-S. thanks the Joachim Herz Foundation for fellowship support. We thank the NCI DTP for NCI60 screening; Ramon Messeguer at Leitat for initial *in vivo* proof of concept studies; Diana Behrens and team at EPO Berlin for followup *in vivo* studies; Anna Kondratiuk, Yuliia Holota, Sergey Zozulya, and the other team members at Bienta (Kyiv, Ukraine) for *in vivo* PK and initial MTD studies; and Bettina

Stahnke, Philipp Metzger, and team at Reaction Biology for further *in vivo* studies.

## ■ ADDITIONAL NOTE

<sup>a</sup>Where quantities are averaged over non-comparable conditions, the geometric mean (logarithmic) is used. For example, IC<sub>50</sub> values 0.25 nM and 1 nM in two cell lines are averaged to 0.5 nM to give a single indicative value; *idem.* for mean reductive index values over, e.g., 55 NCI cell lines.

## ■ REFERENCES

- (1) Quinney, S. K.; Sanghani, S. P.; Davis, W. I.; Hurley, T. D.; Sun, Z.; Murry, D. J.; Bosron, W. F. Hydrolysis of Capecitabine to 5'-Deoxy-5-Fluorocytidine by Human Carboxylesterases and Inhibition by Loperamide. *J. Pharmacol. Exp. Ther.* **2005**, *313* (3), 1011–1016.
- (2) Peters, C.; Brown, S. Antibody-Drug Conjugates as Novel Anti-Cancer Chemotherapeutics. *Biosci. Rep.* **2015**, *35* (4), No. e00225.
- (3) Seddon, B.; Kelland, L. R.; Workman, P. Bioreductive Prodrugs for Cancer Therapy. In *Suicide Gene Therapy: Methods and Reviews*; Springer, C. J., Ed.; Methods in Molecular Medicine; Humana Press: Totowa, NJ, 2004; pp 515–542. DOI: 10.1385/1-59259-429-8:515.
- (4) Phillips, R. M.; Hendriks, H. R.; Peters, G. J. on behalf of the EORTC-Pharmacology and Molecular Mechanism Group. EO9 (Apaziquone): From the Clinic to the Laboratory and Back Again: Preclinical and Clinical History of EO9. *Br. J. Pharmacol.* **2013**, *168* (1), 11–18.
- (5) Furman, R. R.; Bartlett, N. L.; Wong, A. F.; McCulloch, L. M.; Lam, G. N.; Rosenthal, T.; Flinn, I.; Leonard, J. P. Banoxantrone (AQ4N), a Tissue Targeted Prodrug: Results of a Phase 1 Study in Lymphomas. *Blood* **2006**, *108* (11), 2429.
- (6) Hay, M. P.; Hicks, K. O.; Pchalek, K.; Lee, H. H.; Blaser, A.; Pruijn, F. B.; Anderson, R. F.; Shinde, S. S.; Wilson, W. R.; Denny, W. A. Tricyclic [1,2,4]Triazine 1,4-Dioxides As Hypoxia Selective Cytotoxins. *J. Med. Chem.* **2008**, *51* (21), 6853–6865.
- (7) Sun, J. D.; Liu, Q.; Wang, J.; Ahluwalia, D.; Ferraro, D.; Wang, Y.; Duan, J.-X.; Ammons, W. S.; Curd, J. G.; Matteucci, M. D.; Hart, C. P. Selective Tumor Hypoxia Targeting by Hypoxia-Activated Prodrug TH-302 Inhibits Tumor Growth in Preclinical Models of Cancer. *Clin. Cancer Res.* **2012**, *18* (3), 758–770.
- (8) McKeage, M. J.; Jameson, M. B.; Ramanathan, R. K.; Rajendran, J.; Gu, Y.; Wilson, W. R.; Melink, T. J.; Tchekmedyan, N. S. PR-104 a Bioreductive Pre-Prodrug Combined with Gemcitabine or Docetaxel in a Phase Ib Study of Patients with Advanced Solid Tumours. *BMC Cancer* **2012**, *12* (1), 496.
- (9) Wilson, W. R.; Denny, W. A.; Twigden, S. J.; Baguley, B. C.; Probert, J. C. Selective Toxicity of Nitracrine to Hypoxic Mammalian Cells. *Br. J. Cancer* **1984**, *49* (2), 215–223.
- (10) Spiegelberg, L.; Houben, R.; Niemans, R.; de Ruyscher, D.; Yaromina, A.; Theys, J.; Guise, C. P.; Smail, J. B.; Patterson, A. V.; Lambin, P.; Dubois, L. J. Hypoxia-Activated Prodrugs and (Lack of) Clinical Progress: The Need for Hypoxia-Based Biomarker Patient Selection in Phase III Clinical Trials. *Clin. Trans. Rad. Oncol.* **2019**, *15*, 62–69.
- (11) Holmgren, A.; Lu, J. Thioredoxin and Thioredoxin Reductase: Current Research with Special Reference to Human Disease. *Biochem. Biophys. Res. Commun.* **2010**, *396* (1), 120–124.
- (12) Arnér, E. S. J. Perspectives of TrxR1-Based Cancer Therapies. In *Oxidative Stress*; Elsevier, 2020; pp 639–667.
- (13) Powis, G.; Kirkpatrick, D. L. Thioredoxin Signaling as a Target for Cancer Therapy. *Curr. Opin. Pharmacol.* **2007**, *7* (4), 392–397.
- (14) Henne, W. A.; Doorneweerd, D. D.; Hilgenbrink, A. R.; Kularatne, S. A.; Low, P. S. Synthesis and Activity of a Folate Peptide Camptothecin Prodrug. *Bioorg. Med. Chem. Lett.* **2006**, *16* (20), 5350–5355.
- (15) Li, X.; Hou, Y.; Meng, X.; Ge, C.; Ma, H.; Li, J.; Fang, J. Selective Activation of a Prodrug by Thioredoxin Reductase Providing a Strategy to Target Cancer Cells. *Angew. Chem., Int. Ed.* **2018**, *57* (21), 6141–6145.
- (16) Felber, J. G.; Poczka, L.; Scholzen, K. C.; Zeisel, L.; Maier, M. S.; Busker, S.; Theisen, U.; Brandstädter, C.; Becker, K.; Arnér, E. S. J.; Thorn-Seshold, J.; Thorn-Seshold, O. Cyclic 5-Membered Disulfides Are Not Selective Substrates of Thioredoxin Reductase, but Are Opened Nonspecifically. *Nat. Commun.* **2022**, *13* (1), 1754.
- (17) Felber, J. G.; Zeisel, L.; Poczka, L.; Scholzen, K.; Busker, S.; Maier, M. S.; Theisen, U.; Brandstädter, C.; Becker, K.; Arnér, E. S. J.; Thorn-Seshold, J.; Thorn-Seshold, O. Selective, Modular Probes for Thioredoxins Enabled by Rational Tuning of a Unique Disulfide Structure Motif. *J. Am. Chem. Soc.* **2021**, *143* (23), 8791–8803.
- (18) Zeisel, L.; Felber, J. G.; Scholzen, K. C.; Poczka, L.; Cheff, D.; Maier, M. S.; Cheng, Q.; Shen, M.; Hall, M. D.; Arnér, E. S. J.; Thorn-Seshold, J.; Thorn-Seshold, O. Selective Cellular Probes for Mammalian Thioredoxin Reductase TrxR1: Rational Design of RX1, a Modular 1,2-Thiaselenane Redox Probe. *Chem* **2022**, *8* (5), 1493–1517.
- (19) Zeisel, L.; Felber, J. G.; Scholzen, K. C.; Schmitt, C.; Wiegand, A.; Komissarov, L.; Arnér, E. S. J.; Thorn-Seshold, O. Bifunctional, Piperazine-Fused Cyclic Disulfides for Oxidoreductase-Activated Cellular Proagents. *ChemRxiv Preprint* **2023**, DOI: 10.26434/chemrxiv-2023-tm21m.
- (20) Zeisel, L.; Maier, M. S.; Thorn-Seshold, O. Efficient and Scalable Syntheses of 1,2-Thiaselenane-4-Amine and 1,2-Thiaselenane-5-Amine. *Synthesis* **2023**, DOI: 10.1055/a-2022-1398.
- (21) Li, L. H.; Swenson, D. H.; Schpok, S. L. F.; Kuentzel, S. L.; Dayton, B. D.; Krueger, W. C. CC-1065 (NSC-298223), a Novel Antitumor Agent That Interacts Strongly with Double-Stranded DNA. *Cancer Res.* **1982**, *42*, 999–1004.
- (22) Felber, J. G.; Thorn-Seshold, O. 40 Years of Duocarmycins: A Graphical Structure/Function Review of Their Chemical Evolution, from SAR to Prodrugs and ADCs. *JACS Au* **2022**, *2*, 2636.
- (23) Boger, D. L.; Hertzog, D. L.; Bollinger, B.; Johnson, D. S.; Cai, H.; Goldberg, J.; Turnbull, P. Duocarmycin SA Shortened, Simplified, and Extended Agents: A Systematic Examination of the Role of the DNA Binding Subunit. *J. Am. Chem. Soc.* **1997**, *119* (21), 4977–4986.
- (24) Boger, D. L.; Ishizaki, T.; Kitos, P. A.; Suntornwat, O. Synthesis of N-(Tert-Butyloxycarbonyl)-CBI, CBI, CBI-CDP11, and CBI-CDP12: Enhanced Functional Analogs of CC-1065 Incorporating the 1,2,9,9a-Tetrahydrocyclopropa[c]Benz[e]Indol-4-One (CBI) Left-Hand Subunit. *J. Org. Chem.* **1990**, *55* (23), 5823–5832.
- (25) Boger, D. L.; Yun, W.; Han, N. 1,2,9,9a-Tetrahydrocyclopropa[c]Benz[e]Indol-4-One (CBI) Analogs of CC-1065 and the Duocarmycins: Synthesis and Evaluation. *Bioorg. Med. Chem.* **1995**, *3* (11), 1429–1453.
- (26) Boger, D. L.; Yun, W. CBI-TMI: Synthesis and Evaluation of a Key Analog of the Duocarmycins. Validation of a Direct Relationship between Chemical Solvolytic Stability and Cytotoxic Potency and Confirmation of the Structural Features Responsible for the Distinguishing Behavior of Enantiomeric Pairs of Agents. *J. Am. Chem. Soc.* **1994**, *116* (18), 7996–8006.
- (27) Nagamura, S.; Kobayashi, E.; Gomi, K.; Saito, H. Synthesis and Antitumor Activity of Duocarmycin Derivatives: A-Ring Pyrrole Analogues of Duocarmycin B2. *Bioorg. Med. Chem.* **1996**, *4* (8), 1379–1391.
- (28) Boger, D. L. CBI Prodrug Analogs of CC-1065 and the Duocarmycins. *Synthesis* **1999**, *1999* (S1), 1505–1509.
- (29) Tietze, L. F.; Major, F.; Schubert, I. Antitumor Agents: Development of Highly Potent Glycosidic Duocarmycin Analogues for Selective Cancer Therapy. *Angew. Chem., Int. Ed.* **2006**, *45* (39), 6574–6577.
- (30) Tietze, L. F.; von Hof, J. M.; Müller, M.; Krewer, B.; Schubert, I. Glycosidic Prodrugs of Highly Potent Bifunctional Duocarmycin Derivatives for Selective Treatment of Cancer. *Angew. Chem., Int. Ed.* **2010**, *49* (40), 7336–7339.
- (31) Atwell, G. J.; Milbank, J. J. B.; Wilson, W. R.; Hogg, A.; Denny, W. A. 5-Amino-1-(Chloromethyl)-1,2-Dihydro-3 H -Benz[e]Indoles: Relationships between Structure and Cytotoxicity for Analogues Bearing Different DNA Minor Groove Binding Subunits. *J. Med. Chem.* **1999**, *42* (17), 3400–3411.

- (32) Tercel, M.; Atwell, G. J.; Yang, S.; Ashoorzadeh, A.; Stevenson, R. J.; Botting, K. J.; Gu, Y.; Mehta, S. Y.; Denny, W. A.; Wilson, W. R.; Pruijn, F. B. Selective Treatment of Hypoxic Tumor Cells In Vivo: Phosphate Pre-Prodrugs of Nitro Analogues of the Duocarmycins. *Angew. Chem., Int. Ed.* **2011**, *50* (11), 2606–2609.
- (33) Jin, W.; Trzupke, J. D.; Rayl, T. J.; Broward, M. A.; Vielhauer, G. A.; Weir, S. J.; Hwang, I.; Boger, D. L. A Unique Class of Duocarmycin and CC-1065 Analogues Subject to Reductive Activation. *J. Am. Chem. Soc.* **2007**, *129* (49), 15391–15397.
- (34) Boger, D. L. CBI Derivatives Subject to Reductive Activation. US 20110112163A1, May 12, 2011.
- (35) Boger, D. L.; Johnson, D. S. CC-1065 and the Duocarmycins: Understanding Their Biological Function through Mechanistic Studies. *Angew. Chem., Int. Ed.* **1996**, *35* (1314), 1438–1474.
- (36) Baird, R.; Winstein, S. Neighboring Carbon and Hydrogen. LI. Dienones from Ar1–3 Participation. Isolation and Behavior of Spiro(2,5)Octa-1,4-Diene-3-One. *J. Am. Chem. Soc.* **1963**, *85*, 567–578.
- (37) Boger, D. L.; Johnson, D. S.; Yun, W.; Tarby, C. M. Molecular Basis for Sequence Selective DNA Alkylation by (+)- and Ent(-)-CC-L065 and Related Agents: Alkylation Site Models That Accommodate the Offset AT-Rich Adenine N3 Alkylation Selectivity. *Bioorg. Med. Chem.* **1994**, *2* (2), 115–135.
- (38) Kitowski, A.; Zeisel, L.; Felber, J. G.; Heise, C.; Thorn-Seshold, J.; Thorn-Seshold, O. Development and in Vivo Characterization of New, Bioreductive SN38 Prodrugs. Manuscript in preparation, 2023.
- (39) Ogasawara, H.; Nishio, K.; Takeda, Y.; Ohmori, T.; Kubota, N.; Funayama, Y.; Ohira, T.; Kuraishi, Y.; Isogai, Y.; Saijo, N. A Novel Antitumor Antibiotic, KW-2189 Is Activated by Carboxyl Esterase and Induces DNA Strand Breaks in Human Small Cell Lung Cancer Cells. *Jpn. J. Cancer Res.* **1994**, *85*, 418–425.
- (40) Dittert, L. W.; Higuchi, T. Rates of Hydrolysis of Carbamate and Carbonate Esters in Alkaline Solution. *J. Pharm. Sci.* **1963**, *52* (9), 852–857.
- (41) Jarho, E. M.; Wallén, E. A. A.; Christiaans, J. A. M.; Forsberg, M. M.; Venäläinen, J. I.; Männistö, P. T.; Gynther, J.; Poso, A. Dicarboxylic Acid Azacycle L-Prolyl-Pyrrolidine Amides as Prolyl Oligopeptidase Inhibitors and Three-Dimensional Quantitative Structure-Activity Relationship of the Enzyme-Inhibitor Interactions. *J. Med. Chem.* **2005**, *48* (15), 4772–4782.
- (42) Frecentese, F.; Fiorino, F.; Perissutti, E.; Severino, B.; Magli, E.; Esposito, A.; De Angelis, F.; Massarelli, P.; Nencini, C.; Viti, B.; Santagada, V.; Caliendo, G. Efficient Microwave Combinatorial Synthesis of Novel Indolic Arylpiperazine Derivatives as Serotoniner-gic Ligands. *Eur. J. Med. Chem.* **2010**, *45* (2), 752–759.
- (43) Hennequin, L. F. A.; Ple, P.; Stokes, E. S. E.; McKercher, D. Quinazoline Derivatives as Angiogenesis Inhibitors. EP 1154774B1, June 22, 2005.
- (44) Giddens, A. C.; Lee, H. H.; Lu, G.-L.; Miller, C. K.; Guo, J.; Lewis Phillips, G. D.; Pillow, T. H.; Tercel, M. Analogues of DNA Minor Groove Cross-Linking Agents Incorporating AminoCBI, an Amino Derivative of the Duocarmycins: Synthesis, Cytotoxicity, and Potential as Payloads for Antibody-Drug Conjugates. *Bioorg. Med. Chem.* **2016**, *24* (22), 6075–6081.
- (45) Butkevich, A. N.; Bossi, M. L.; Lukinavičius, G.; Hell, S. W. Triarylmethane Fluorophores Resistant to Oxidative Photobleaching. *J. Am. Chem. Soc.* **2019**, *141* (2), 981–989.
- (46) Li, L. H.; DeKoning, T. F.; Kelly, R. C.; Krueger, W. C.; McGovern, J. P.; Padbury, G. E.; Petzold, G. L.; Wallace, T. L.; Ouding, R. J.; Prairie, M. D.; Gebhard, I. Cytotoxicity and Antitumor Activity of Carzelesin, a Prodrug Cyclopropylpyrroloindole Analogue. *Cancer Res.* **1992**, *52*, 4904–4913.
- (47) Wang, Y.; Li, L.; Tian, Z.; Jiang, W.; Larrick, J. W. Synthesis and Antitumor Activity of CBI-Bearing Ester and Carbamate Prodrugs of CC-1065 Analogue. *Bioorg. Med. Chem.* **2006**, *14* (23), 7854–7861.
- (48) Sato, A.; McNulty, L.; Cox, K.; Kim, S.; Scott, A.; Daniell, K.; Summerville, K.; Price, C.; Hudson, S.; Kiakos, K.; Hartley, J. A.; Asao, T.; Lee, M. A Novel Class of in Vivo Active Anticancer Agents: Achiral *Seco*-Amino- and *Seco*-Hydroxycyclopropylbenz[e]Indolone (*Seco*-CBI) Analogues of the Duocarmycins and CC-1065. *J. Med. Chem.* **2005**, *48* (11), 3903–3918.
- (49) Mandal, P. K.; Schneider, M.; Kölle, P.; Kuhlencordt, P.; Förster, H.; Beck, H.; Bornkamm, G. W.; Conrad, M. Loss of Thioredoxin Reductase 1 Renders Tumors Highly Susceptible to Pharmacologic Glutathione Deprivation. *Cancer Res.* **2010**, *70* (22), 9505–9514.
- (50) Du, Y.; Zhang, H.; Lu, J.; Holmgren, A. Glutathione and Glutaredoxin Act as a Backup of Human Thioredoxin Reductase 1 to Reduce Thioredoxin 1 Preventing Cell Death by Aurothioglucose. *J. Biol. Chem.* **2012**, *287* (45), 38210–38219.
- (51) Shoemaker, R. H. The NCI60 Human Tumour Cell Line Anticancer Drug Screen. *Nat. Rev. Cancer* **2006**, *6* (10), 813–823.
- (52) Pulaski, B. A.; Ostrand-Rosenberg, S. Mouse 4T1 Breast Tumor Model. *Current. Protoc. Immunol.* **2000**, *39* (1), 20.2.1–20.2.16.
- (53) Tan, M. H.; Nowak, N. J.; Loor, R.; Ochi, H.; Sandberg, A. A.; Lopez, C.; Pickren, J. W.; Berjian, R.; Douglass, H. O.; Chu, T. M. Characterization of a New Primary Human Pancreatic Tumor Line. *Cancer Invest.* **1986**, *4* (1), 15–23.
- (54) Deer, E. L.; González-Hernández, J.; Coursen, J. D.; Shea, J. E.; Ngatia, J.; Scaife, C. L.; Firpo, M. A.; Mulvihill, S. J. Phenotype and Genotype of Pancreatic Cancer Cell Lines. *Pancreas* **2010**, *39* (4), 425–435.